Indian Journal of Science and Technology, Vol 9(30), DOI: 10.17485/ijst/2016/v9i30/99275, August 2016
ISSN (Print) : 0974-6846
ISSN (Online) : 0974-5645

Evaluating the Impact of SNOIs on SINR and Beampattern of MVDR Adaptive Beamforming Algorithm

Suhail Najm Shahab[1*], Ayib Rosdi Zainun[1], Izzeldin Ibrahim Mohamed[1], Waleed M. Sh. Alabdraba[2] and Nurul Hazlina Noordin[1]

[1]Faculty of Electrical and Electronics Engineering, Universiti Malaysia Pahang, 26600, Pahang, Malaysia; 68suhel@gmail.com
[2]Enviromental Engineering Department, College of Engineering, Tikrit University, Iraq

Abstract

Minimum Variance Distortionless Response (MVDR) is basically a unity gain adaptive beamformer which is suffered from performance degradation due to the presence of interference and noise. Also, MVDR is sensitive to errors such as the steering vector errors, and the nulling level. MVDR combined with a Linear Antenna Array (LAA) is used to acquire desired signals and suppress the interference and noise. This paper examines the impact of the number of interference sources and the mainlobe accuracy by using Signal to Interference plus Noise Ratio (SINR) and array beampattern as two different Figure-of-Merits to measure the performance of the MVDR beamformer with a fixed number of array elements (L). The findings of this study indicate that the MVDR successfully form a nulls to L-1 nonlook signal with average SINR of 49.31 dB. Also, the MVDR provides accurate mainlobe with a small change to the real user direction when the SNOIs are bigger than array elements. The proposed method was found to perform better than some existing techniques. Based on this analysis, the beampattern not heavily relies on the number of unwanted source. Moreover, the SINR strongly depends on the number of SNOIs and the nulling level.

Keywords: Beamforming, Linear Antenna Array, Minimum Variance Distortionless Response, SINR, Smart Antenna

1. Introduction

Currently, the mobile cellular networks are experiencing a massive evolution of data traffic, because of multimedia and internet applications that are used by a vast number of devices such as smartphones, mobile PC and tablets[1,2]. Most beamforming techniques have been considered for use at the Base Station (BS) since antenna arrays are not feasible at mobile terminals due to space limitations[3].

The Long Term Evolution (LTE), as introduced by the 3rd Generation Partnership Project (3GPP), is an extremely flexible radio interface, the first LTE deployment was in 2011. LTE is the evolution of 3GPP Universal Mobile Telecommunication System (UMTS) towards an all-IP network to ensure the competitiveness of UMTS for the next ten years and beyond. LTE was developed in Release 8 and 9 of the 3GPP specification. Maravedis, anticipates that 3 LTE–TDD and 59 LTE–FDD networks will be running worldwide by the end of 2011. By 2016, there will be 305 million LTE subscribers, which means about 44 million (14%) will be LTE–TDD clients and the remaining 261 million (86%) will be LTE–FDD[4]. With the increasing trend of he number of subscribers and demand for different services in wireless systems, there are always requirements for better coverage, higher data rate, improved spectrum efficiency and reduced operating cost. To fulfill this requirement, beamforming technique is able to focus the array antenna pattern into a particular direction and thereby enhances the desired signal power.

Interference is one of the significant obstacles in the wirel-ess networks. It can be caused by other users or by the signal itself[5]. The signal can interfere with itself

*Author for correspondence

due to multipath components, where the signal is gathered with another versi-on of the signal that is delayed because of another propagati-on path[6]. The fundamental principle of the Adaptive Beamforming (ABF) algorithm is to track the statistics of the surrounding interference and noise field as well as adaptively placing nulls that decrease dramatically the interference and noise under the restriction that the look angle is not distorted at the beamformer's output[7]. The basic idea of the Minim-um Variance Distortionless Response (MVDR) algorithm is to estimate the beamforming excitation coefficients in an adaptive way by minimizing the variance of the residual inte-rference and noise whilst enforcing a set of linear constraints to ensure that the real user signal are not distorted[7].

The authors in[8] proposed an enhanced model of MVDR algorithm by replace the position of the reference element in steering vector to be in the central of the array and the number of elements must be odd. Simulation results show that modified MVDR has a realistic behavior especially for detecting the incoming signals direction and outperforms the conventional MVDR. One of the popular approaches to improve the classic Capon beamformer in the presence of finite sample effect and steering vector errors is the diagonal loading, which was studied by[9]. The idea behind diagonal loading is to adapt a covariance matrix by adding a displacement value to the diagonal elements of the estimated covariance matrix. Nevertheless, how to select an appropriate diagonal loading level is a challenging task. In[10] mentioned that the element spacing must be interelement $\leq \lambda/2$ to prevent spatial aliasing. In[11], the author presents a comparative study of MVDR algorithm and LMS algorithm, where results show that LMS is the better performer. The SINR maximization is another criterion employed in the joint transmitter and receiver beamforming algorithms[12–14]. In an analysis of, the mixing of differential algorithm based LAA is applied to deepen nulls and lower Side Lobe Levels (SLLs) in the unwanted direction, and they found the max null depth of -63 dB by using 20 element. The statistic numerical algorithm was proposed to obtain the requirement for the amplitude and phase error of multibeam active phased array antenna[16]. The radiation beampattern is simulated from the value of the random amplitude and phase errors of phase shifter. From the results, it is found that the only way to meet the requirement of the sidelobe level is to use Digital Beamforming (DBF). The researchers in[7] investigate the performance of the MVDR beamformer for four different types of noise and source incidence angles using SNR and beampattern as the evaluation criteria. An evaluation of the trade-off between noise reduction and reverberation of the MVDR filter is presented in[17]. More recent study in[18] compares the MVDR and Delay and Sum (DAS) beamformer by using different matrix inverse method. The finding proved that the MVDR outperform DAS through FPGA implementation with narrow mainlobe beamwidth and lower sidelobe level.

Smart Antennas (SA) include signal processing capabilities that perform tasks such as the Direction of Arrival (DOA) estimation and beamforming. A smart antenna that is held in the Base Station (BS) of a cellular network consists of antenna arrays where the output power are accustomed by a group of weight vectors using an ABF algorithm. Before ABF, the DOA estimation is used to specify the main directions of all incoming signals. A previous research has analyzed the accuracy and precision of a proposed wideband capon beamforming for estimating the elevation angle, azimuth angle and velocity for target parameters using planner antenna array[19]. The function of ABF algorithms is to form the mainbeam to the user direction and placing nulls towards interference and noise directions by adjusting the antenna itself using beamforming (BF) techniques to achieve better transmission or reception beampattern which increases SINR by mitigating co-channel interference present in the wireless communication system. The ABF algorithm improves the output of the array beampattern in a way which it maximizes the radiated power where it will be produced in the wanted users direction. Moreover, deep nulls are placed in the unwanted signal directions that symbolize co-channel interference from desired users in the neighboring BSs.

So far, ABF is a function of the number of unwanted signals and the angular separation between desired user and undesired signals. Therefore, it is important to investigate the impact of SNOIs on the beampattern that can offer the best BF capabilities in terms of directing the mainlobe toward the Signal of Interest (SOI) direction while nulls towards the Signal Not of Interest (SNOI) direction. In this paper, for a fixed number of antenna elements, in order to evaluate the performance of the MVDR algorithm applied to the ABF problem of LAA, the scenarios proposed are mainly presented in terms of extremely adverse conditions, i.e., by increasing the unwanted source to exceed the number of array elements over which the array antenna span whilst precisely steering the mainbeam toward the specified direction with

an isolation from the null, and by rejecting interference presented on the array system. Whereas no complete assessment of the SINR and the beampattern as a function of all the above mentioned parameters. The analysis of the MVDR in this work is carried out in three different scenarios where the MVDR performance is assessed with two important metrics; SINR and beampattern. This investigation not only helps to better figure out the MVDR beamformer, but also helps to form a better array system in real-world application. The remainder of this paper is organized as follows. In Section 2, MVDR beamformer based on linear antenna array design method with the signal propagation model is described. The simulation results and performance analysis are provided in Section 3. Finally, in Section 4, the paper's conclusions and summary of MVDR performance are described.

2. System Model and MVDR Beamforming

In this section, the mathematical formulation of the design model for adaptive beamforming will be presented in detail. Consider a single cell with *L* elements antenna array. Let there be *S* wanted signal sources and *I* interference sources spreading on same the frequency channel at the same time. The algorithm starts by creating a real life signal model. A number of plane waves are considered from *K* narrowband sources impinging from various angles (θ, φ). The impinging radio frequency signal reaches into antenna array from far field to the array geometry of Linear Antenna Arrays (LAAs). A block diagram of the antenna array using DOA and BF process is shown in Figure 1. As displayed in this figure 1, after the signals are received by antenna arrays consisting of the wanted user signal, the interference source, and the noise, the first part is to estimate the direction of the arrival of the *S* signal and *I* signals using a well-known algorithm developed by capon, named MVDR spectrum estimator, to find the DOA angles of several sources. However, the MVDR estimator algorithm wants information of the number of sources. With the known direction of the source, then the second part is applied by using MVDR ABF technique that places a straight beam to *S* signal and placing nulls in the direction of *I* signals. Each signal is multiplied by adaptable complex weights and then summed to form the system output.

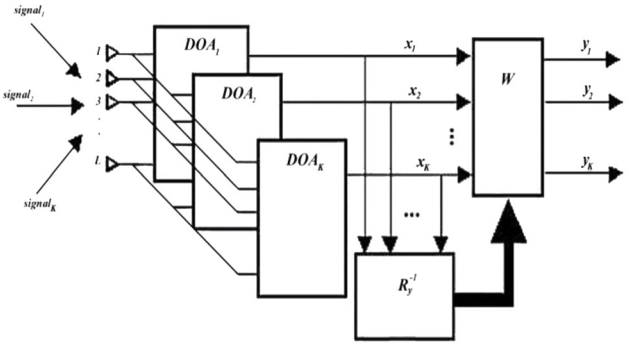

Figure 1. A smart antenna array system using DoA and beamforming process.

The total composite signals received by an adaptive antenna array at time index, t, become:

$$x_T(t) = \sum_{s=1}^{S} x_s(t) + \sum_{i=1}^{I} x_i(t) + x_n \quad (1)$$

$$= \sum_{s=1}^{S} x_s(t)\, a(\theta_s) + \sum_{i=1}^{I} x_i(t)\, a(\theta_i) + x_n \quad (2)$$

Where $x_T(t) \in C^{K\times L}$, $x_s(t)$, $x_i(t)$, $x_n(t)$, denote the desired signal, interference signal and noise added from White Gaussian noise, respectively. The unwanted signal consists of $x_i(t)+x_n(t)$ and *I* is the number of interferences, the desired angle and interference direction of arrival angles are θ_s and θ_i , *i=1,2….,I,* respectively. $a(\theta_s)$ denote the steering vector or array response for wanted signal while $a(\theta_i)$ refers to the interference signal steering vector or array response to the unwanted signal.

Steering vector is a complex vector $\in C^{L\times K}$ containing responses of all elements of the array to a narrowband source of unit power depending on the incident angle, which is given by[20]:

$$a(\theta_{s,i}) = \begin{bmatrix} 1 \\ e^{-jqd\sin\theta_{s,i}} \\ e^{-j\,2d\sin\theta_{s,i}} \\ \vdots \\ e^{-j(L-1)d\sin\theta_{s,i}} \end{bmatrix} \quad (3)$$

Where j is the imaginary unit, (i.e., $j^2 = -1$), *d* is the spacing between elements and *q* is the wave number given as:

$$q = \frac{2\pi}{\lambda} \quad (4)$$

Where λ refers to the received signal wavelength. The signal $x_T(t)$ received by multiple antenna elements is multiplied with a series of amplitude and phase (weight vector coefficients) which accordingly adjust the amplitude and phase of the incoming signal. This weighted signal is a linear combination of the data at L elements, resulting in the array output, $y(t)$ at any time t, of a narrowband beamformer, which is given by;

$$y(t) = \sum_{l=1}^{L} w^H x_T(t) \tag{5}$$

where $y(t)$ is the beamformer output, $x_T(t)$ is the antenna element's output, w is the complex weight vector for the antenna element = $[w_1, w_2, \ldots, w_L]^T$ is $\in C^{L\times 1}$ beamforming complex vector. $(.)^H$ and $(.)^T$ denotes the conjugate transpose (Hermitian transpose) of a vector or a matrix, which is used to simplify the mathematical notation and transposes operators respectively. The weight vector at time t + 1 for any system that uses the immediate gradient vector ∇ξ (t) for weight vector upgrading and evades the matrix inverse operation, which is defined as follows:

$$W(t+1) = W(t) + \frac{1}{2}\mu[\nabla\xi(t)] \tag{6}$$

where μ is the step size parameter, the convergence speed control by μ and lies between 0 and 1. The smallest values of μ facilitate the high-quality estimation and sluggish concurrence, while huge values may result in a rapid union. However, the constancy over the minimum value may disappear. Consider

$$0 < \mu < 1/\lambda \tag{7}$$

An instantaneous estimation of gradient vector is written as

$$\nabla\xi(t) = -2p(t) + 2R_y(t)W(t) \tag{8}$$

$$p(t) = d^*(t)x_T(t) \tag{9}$$

$$R_y = x_T(t){x_T}^H(t) \tag{10}$$

A precise calculation of ∇ξ(t) is not possible because prior information on cross-correlation vector, p and covariance matrix, R_y of the measurement vector are required. By substituting Equation (8) with Equation (6), the weight vector is derived as follows:

$$\begin{aligned} W(t+1) &= W(t) + \mu[p(t) - R(t)W(t)] \\ &= W(t) + \mu x_T(t)[d^*(t) - x_T(t)W(t)] \\ &= W(t) + \mu x_T e^*(t) \end{aligned} \tag{11}$$

The following three formulas can further define the desired signal:

$$y(t) = w^H(t)x_T(t) \tag{12}$$

$$\begin{aligned} e(t) &= d(t)\, y(t)W(t+1) \\ &= W(t) + \mu x_T(t)e^*(t) \end{aligned} \tag{13}$$

The covariance matrix, R_y is constructed conventionally with unlimited snapshots. However, it is estimated by using limited snapshots signal in the actual application. It can be expressed as:

$$R_y = \sum_{s=1}^{S}\sigma_s^2 a(\theta_s)a^H(\theta_s) + \sum_{i=1}^{I}\sigma_i^2 a(\theta_i)a^H(\theta_i) + \sigma_n^2 Id_L \tag{14}$$

$$R_s = \sigma_s^2 a(\theta_s)a^H(\theta_s) \tag{15}$$

$$R_{i+n} = \sum_{i=1}^{I}\sigma_i^2 a(\theta_i)a^H(\theta_i) + \sigma_n^2 Id_L \tag{16}$$

$$R_y = R_s + R_{i+n} = \mathrm{E}[x_T(t){x_T}^H(t)] \tag{17}$$

$$\sigma_s^2 = E[|x_s(t)|^2] \tag{18}$$

$$\sigma_i^2 = E[|x_i(t)|^2] \tag{19}$$

where $R_y, \sigma_s^2, \sigma_i^2, \sigma_n^2$, Id_L, R_s, R_{i+n} and $E[.]$ denotes, respectively, the $L\times L$ theoretical covariance matrix, power of the desired signal, interference power, noise power, $L\times L$ identity matrix, *SOI* covariance matrix, interference plus noise covariance matrix and expectation operator.

The most common formulation of the MVDR beamformer that determines the $L\times 1$ optimum weight vector is the solution to the following constrained problem[21]:

$$W_{MVDR} = \arg_{W_{MVDR}} \min(W^H R_y W) = \min \mathrm{E}[|y(t)|^2]$$

$$\Rightarrow \min_w P(\theta) = \{w^H R_y w\} \quad s.t. \quad w^H a(\theta_s) = 1 \tag{20}$$

where $P(\theta)$denotes the mean output power, a beampattern can be given in dB as[22]:

$$beampattern = 20\log_{10}\frac{|P(\theta)|}{\max|P(\theta)|} \tag{21}$$

This method reduces the contribution of the unwanted signal by minimizing the power of output noise and interference and ensuring the power of useful signal equals to 1 (constant) in the direction of useful signal $w^H a(\theta_s)=1$. By using Lagrange multiplier, the MVDR weight vector that gives the solution for the above equation as per the following formula[23]:

$$w_{\text{MVDR}} = \frac{R_y^{-1} a(\theta_s)}{a^H(\theta_s) R_y^{-1} a(\theta_s)} \quad (22)$$

Inserting Equation (22) into Equation (12), the output of MVDR is given by;

$$\begin{aligned} y(t) &= w^H(t)\, x_T(t) \\ &= w^H a(\theta_s)\, x_s(t) + w^H x_i(t)\, a(\theta_i) + w^H x_n \\ &= x_s(t) + w^H x_i(t)\, a(\theta_i) + w^H x_n \end{aligned} \quad (23)$$

The output signal power of the array as a function of the DOA estimation, using optimum weight vector from MVDR beamforming method[24], it is given by MVDR spatial spectrum for angle of arrival estimated by detecting the peaks in this angular spectrum as[25]:

$$P_{MVDR}(\theta) = \frac{1}{a^H(\theta_s) R_y^{-1} a(\theta_s)} \quad (24)$$

Finally, the SINR is defined as the ratio of the desired signal power divided by the undesired signal power:

$$SINR = \frac{\mathrm{E}\{|y_s(t)|^2\}}{\mathrm{E}\{|y_{i+n}(t)|^2\}} = \frac{w^H R_s w}{w^H R_{i+n} w} \quad (25)$$

3. Simulation Results and Analysis

In this study, the performance of the proposed MVDR beamformer method is presented, and illustrative for the array of L linear antenna elements configuration is arranged along some axis added to the beamformer system at the cellular Base Station (BS). The array receives signals from different spatially separated users. The received signal consists of the intended signal, co-channel interference, and a random noise component. To increase the output power of the desired signal and reduce the power of Co-channel interference and noise, beamforming is employed at the BS. The antenna array elements separated by inter-element spacing, d, at carrier frequency (*Fc*) of 2.6 GHz, which is the spectrum band allocated to LTE operators in Malaysia[26]. To measure the performance of the MVDR algorithm for ABF applications with varying number of SNOIs, nulling accuracy to the interference source. The goal is to analyze the effects of intefereing signals to achieve the best beamforming capabilities that form the mainbeam in the wanted direction and null in the directions of interference with highest output SINR.

The incident fields are assumed to impinge from the direction angles $\theta_s = 0°$ and $\theta_i = \{1, 2, \ldots, L+1\}$ in the azimuth plane ($-\pi/2 < \theta < \pi/2$). Throughout the simulations, the array is illuminated by uncorrelated sources of equally power levels. Three different scenarios are considered, and the simulation parameters setting in this study is shown in Table 1.

Table 1. Key simulation parameters of MVDR beamformer

Key System Parameters	Values
Array antenna configuration	LAA
Antenna type	Isotropic
Carrier frequency (Fc)	2.6 GHz
Beam scanning range	±90° (Azimuth)
Number of element (L)	8
Element spacing (d)	λ/2
# SOI	1
# SNOIs	1 : 9
SNR [dB]	10
INR [dB]	10
Snapshots (ns)	250

3.1 The First Scenario

Using multiple antennas at the BS can reduce the effects of co-channel interference, multipath fading, and background noise. Many BF algorithms have been devised to cancel interference sources that appear in the cellular system. MVDR algorithm can null the interferences without any distortion to the real user path.

The first simulation scenario reveals the results calculated by considering the distance between array elements set to be $d=0.5\lambda$ with Signal to Noise Ratio (SNR) = Interference to Noise Ratio (INR) = 10 dB and number of data sample = 250. Figures 2 and 3 illustrates a typical 2D MVDR beampa-ttern plot displayed in a rectangular and polar coordinates, Uniform LAA with $L = 8$ elements, the additive noise is modeled as a complex zero mean white Gaussian noise. Four interfering sources are assumed to have DOAs (θ_i) at ±15° and ±30° respectively.

The SOI is considered to be a plane wave from the presumed direction θ_s = 0°. With the reference element in the one-end side of the array. The graph observes that the MVDR successfully form nulls at each of the interference sources, and it provides maximum gain to the real user direction of the SOI. In case of four interference sources, the deep null of -66.4 dB compared to -48.5 dB for 16 elements was found for a study conducted by[27] based on conjugate gradient method ABF algorithm. Also, the MVDR was capable to form the mainlobe to reach wanted user direction even for the closest interference to the user, which is the same result obtained by using enhanced the MVDR model proposed by[8]. The MVDR weight vector (wMVDR), the Phase shifted for the desired direction (θ_s shift), Peak Side Lobe (PSL) that is closest to the mainbeam, maximum depth null (Null) at interference direction and output SINR are shown in Table 2.

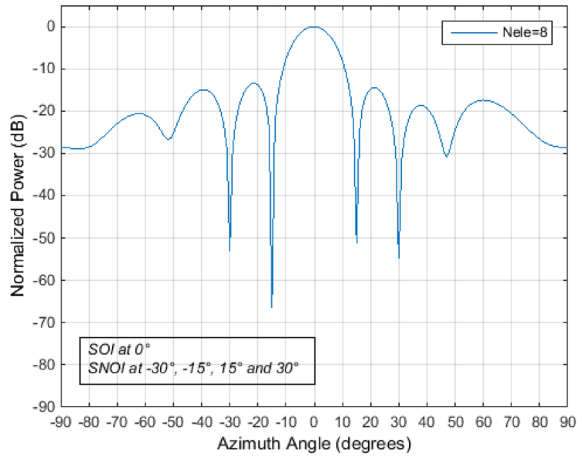

Figure 2. Line plot – beampattern analysis of MVDR with L= 8, d = λ/2 and SNOIs = 4.

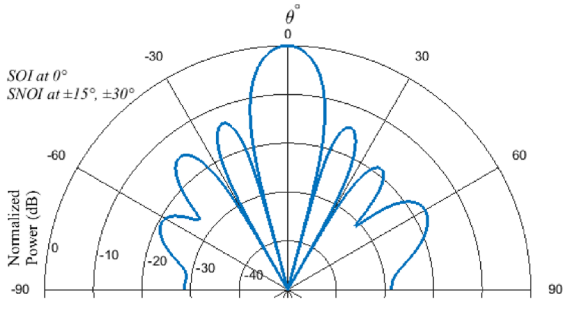

Figure 3. Polar plot – beampattern analysis of MVDR with L = 8, d = λ/2 and SNOIs = 4.

3.2 The Second Scenario

The subsequent MVDR pattern plots with cancelation for all interferences are shown in Figures 4 and 5. It shows

Table 2. MVDR performance analysis for SOI at 0° and SNOIs at ±15° and ±30°

w MVDR	θ_s shift	PSL [dB]	Null [dB]	SINR [dB]
0.1203+0.0088i 0.1267-0.0043i 0.1171-0.0031i 0.1470+0.0111i 0.1215-0.0117i 0.1327+0.0067i 0.1234+0.0007i 0.1112-0.0081i	0	14.1	-66.4	47.9

Table 3. MVDR performance analysis for SOI at 0° and SNOIs at ±15°, ±30°, ±50° and -83°

w MVDR	θ_s shift	PSL [dB]	Null [dB]	SINR [dB]
0.1141-0.0012i 0.1278+0.0017i 0.1218-0.0022i 0.1355+0.0011i 0.1360-0.0002i 0.1231+0.0000i 0.1270-0.0010i 0.1147+0.0016i	0	13.9	-58.1	43.3

the beampattern for an eight-element linear array in the presence of a different Angle of Arrival (AoA) for SOI and SNOIs. The second simulation scenario demonstrates the MVDR behavior when the number of SNOIs increases. Whereas, the performances of the MVDR method are examined in the case of SNOI equal to L-1 interfering source. It is assumed that eight sources impinge on the array of the directions for an SOI at θ_s = 0° and SNOIs (θ_i) at ±15°, ±30°, ±50° and 83° in the azimuth plane. All other parameters are chosen the same in the previous scenario. It is found that the mainlobe still directed to the real user direction with power of 0 dB and the PSL slightly goes up as SNOIs increases while the null-forming level and SINR are strongly affected by SNOIs increases. In other words, sharper and deeper nulls would be produced and hence improve the SINR by adding more elements to the array. In addition, Table 3 compares the power values of SINR for seven interfering signals with corresponding MVDR weight vector. Moreover, increasing the number of elements results in narrower mainlobe beamwidth that is very useful in directing the antenna beam to the desired user while the number of nulls in the pattern increases. On the other hand, the computing operations become more complex. Besides, as the number of array sen-

sors increases, the mean cost of design increases due to the increasing number of RF modules, A/D converters, and other components. This causes the operational power consumption to increase as well.

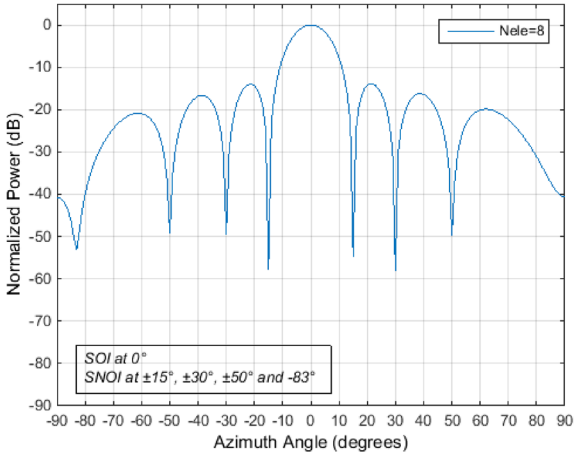

Figure 4. Line plot – beampattern analysis of MVDR with L = 8, d = λ/2 and SNOIs = 7.

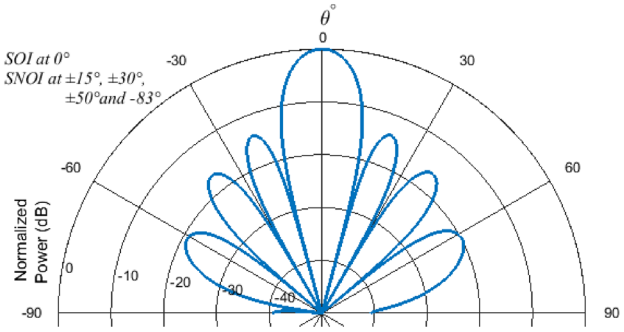

Figure 5. Polar plot – beampattern analysis of MVDR with L= 8, d = λ/2 and SNOIs = 7.

3.3 The Third Scenario

This scenario is done to show how MVDR beamformer deal with interference source in case of having SNOIs > L on the performance of MVDR for a desired user at θ_s = 0° and nine interference signals (θ_i) at ±15°, ±30°, ±50°, 60° and ±80° with L = 8, d = λ/2. Figure 6 and 7 displays the antenna patterns steered to real user source angle with the interference signal > L, it gives the output beampattern with seven nulls due to the antenna array able to provide a null of L-1 with one degree of freedom. It can be seen that the MVDR shows null at direction ±15°, ±30°, ±50°, 80° with output SINR equal to 22.1 dB with mainlobe shape is unaffected as depicted in Table 4. In this manner, MVDR beamformer found to cancel L-1 interference source. In short, reducing the effect of interference arriving outside the mainlobe. This interference reduction increases the capacity of the communication systems. Pattern nulling at specific directions suppresses the interference from other sources located at these directions.

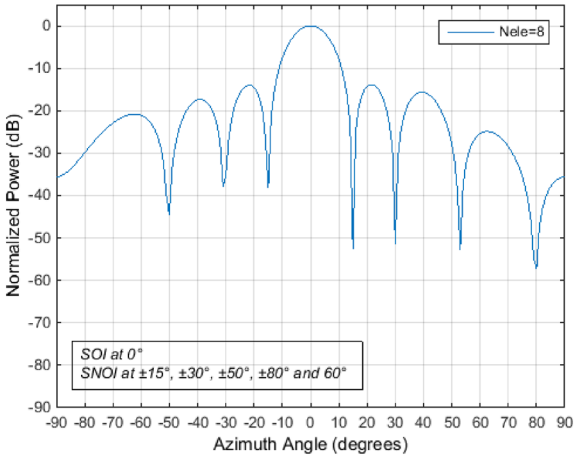

Figure 6. Line plot – beampattern analysis of MVDR with L = 8, d = λ/2 and SNOIs = 9.

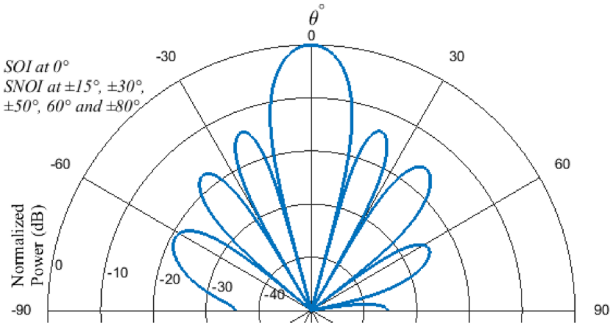

Figure 7. Polar plot – beampattern analysis of MVDR with L = 8, d = λ/2 and SNOIs = 9.

Table 4. MVDR performance analysis for SOI at 0° and SNOIs at ±15°, ±30°, ±50°, 60 ° and ±80°

w MVDR	θ_s shift	PSL [dB]	Null [dB]	SINR [dB]
0.1092+0.0002i 0.1330+0.0026i 0.1201+0.0029i 0.1372-0.0067i 0.1372+0.0070i 0.1204-0.0047i 0.1333-0.0018i 0.1095+0.0004i	-0.005	14.3	-57.1	22.1

The graph in Figure 8 compares the SINR of the MVDR beamformer for various interference sources at a given background noise starting from I = 1 and

until L+1 for the fixed number of elements. It can be clearly seen that the SINR values for SNOI ≤ L-1 is nearly above 43.39 dB. Whereas, the SINR is heavily decreased as the undesired sources exceed the number of array elements. Finally, in terms of required computational time, it is found that the required processing time for MVDR increases against the number of SNOIs increase as displayed in Figure 9. For example, when the number of signals ≤ L it required about 0.75 second to get the final results compared to 0.91 second for signals ≥ L. This simulation was operated on Intel® Core 2 Due CPU @ 3.0GHz, 4GB RAM runs on Windows 7 64bit operating system.

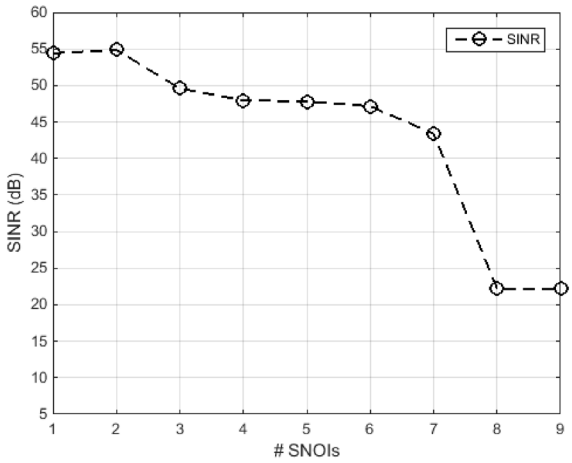

Figure 8. SINR vs #SNOIs with L = 8, d = λ/2.

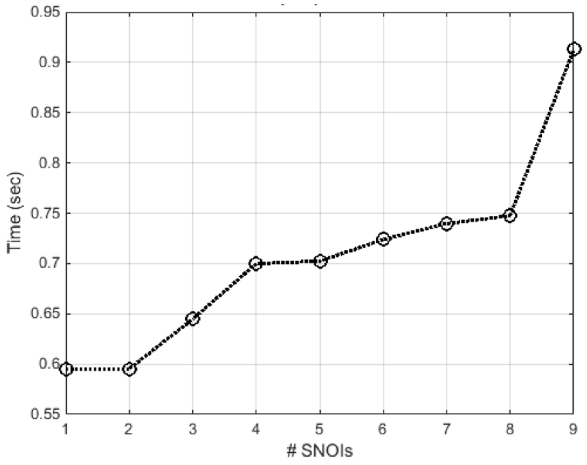

Figure 9. Processing time vs #SNOIs.

4. Conclusions

MVDR algorithm that has gained significance in the wireless cellular communication system due to its capability to suppress co-channel and adjacent channel interferences and raised SINR helps to improve system capacity. A number of computer simulations were performed with different numbers of interference sources with varying angular separations between SOI and SNOI. The results obtained using MVDR algorithm has the best beam formed pattern in suppressing the interference and noise reduction with accurate mainlobe to look angle of the desired direction when there are interference sources less than the number of array elements due to antenna array system able to null (L-1) of unwanted source. MVDR shows the capability of null-forming towards the unwanted signals with negative power, and high accuracy even in the case of multiple interferences. The MVDR performance, reduces as the interference sources are increased. The computation time can be further decreased if higher signal processor is used. An ongoing research extends the results of this paper to enhance MVDR algorithm.

5. Acknowledgment

This research was supported by Universiti Malaysia Pahang, through the Fundamental Research Grant Scheme (FRGS) funded by the Ministry of Education (RDU 140129).

6. References

1. Cisco Visual Networking Index. Global mobile data traffic forecast update, 2013–2018. San Jose, CA, USA: Cisco Systems Inc; 2014.
2. Ericsson Mobility Report. On the Pulse of the Networked Society. Kista, Sweden: Ericsson; 2015.
3. Liberti JC, Rappaport TS. Smart antennas for wireless communications: IS-95 and third generation CDMA applications. Prentice Hall PTR; 1999.
4. Garza C. 4G digest - 17.25 million BWA/WiMAX and 320 thousand LTE subscribers reached in Q1 2011 4G Digest; 2011.
5. Halim MA. Adaptive array measurements in communications. 1st ed. Norwood, MA, USA: Artech House Publichers; 2001.
6. Okkonen J. Uniform linear adaptive antenna array beamforming implementation with a wireless open-access research platform. University of Oulu; 2013 May.
7. Pan C, Chen J, Benesty J. Performance study of the MVDR beamformer as a function of the source incidence angle. IEEE/ACM Transactions on Audio, Speech, and Language Processing. 2014; 22(1):67–79.

8. Khaldoon AO, Rahman MM, Ahmad RB, Hassnawi LA. Enhanced uniform linear array performance using modified minimum variance distortionless response beamformer algorithm. 2nd International Conference on Electronic Design (ICED); 2014. p. 198–203.
9. Lin J-R, Peng Q-c, Shao H-z. On diagonal loading for robust adaptive beamforming based on worst-case performance optimization. ETRI Journal. 2007 Feb; 29(1):50–8.
10. Manolakis DG, Ingle VK, Kogon SM. Statistical and adaptive signal processing: Spectral estimation, signal modeling, adaptive filtering, and array processing. Norwood, MA, USA: Artech House Inc; 2005.
11. Das KJ, Sarma KK, editors. Adaptive beamforming for efficient interference suppression using minimum variance distortionless response. International Conference on Advancement in Engineering Studies and Technology; 2012.
12. Choi RL-U, Murch RD, Letaief K. MIMO CDMA antenna system for SINR enhancement. IEEE Transactions on Wireless Communications. 2003; 2(2):240–9.
13. Serbetli S, Yener A. Transceiver optimization for multiuser MIMO systems. IEEE Transactions on Signal Processing. 2004; 52(1):214–26.
14. Kum D, Kang D, Choi S. Novel SINR-based user selection for an MU-MIMO system with limited feedback. ETRI Journal. 2014; 36(1):62–8.
15. Rao AP, Sarma N. Performance analysis of differential evolution algorithm based beamforming for smart antenna systems. IJWMT. 2014; 4(1):1–9.
16. Ku B-J, Ahn D-S, Lee S-P, Shishlov A, Reutov A, Ganin S, et al. Radiation pattern of multibeam array antenna with digital beamforming for stratospheric communication system: Statistical simulation. ETRI Journal. 2002; 24(3):197–204.
17. Habets E, Benesty J, Cohen I, Gannot S, Dmochowski J. New insights into the MVDR beamformer in room acoustics. IEEE Transactions on Audio, Speech, and Language Processing. 2010; 18(1):158–70.
18. Hema N, Kidav JU, Lakshmi B. VLSI architecture for broadband MVDR beamformer. Indian Journal of Science and Technology. 2015; 8(19).
19. Lee M-S. Wideband Capon beamforming for a planar phased radar array with antenna switching. ETRI Journal. 2009; 31(3):321–3.
20. Godara LC. Smart antennas. Boca Raton: CRC press; 2004.
21. Souden M, Benesty J, Affes S. A study of the LCMV and MVDR noise reduction filters. IEEE Transactions on Signal Processing. 2010; 58(9):4925–35.
22. Godara LC. Application of antenna arrays to mobile communications. II. Beam-forming and direction-of-arrival considerations. Proceedings of the IEEE. 1997; 85(8):1195–245.
23. Renzhou G, editor Suppressing radio frequency interferences with adaptive beamformer based on weight iterative algorithm. Conference on Wireless, Mobile and Sensor Networks, (CCWMSN07), IET; 2007.
24. Haykin S. Adaptive filter theory. 4th ed: Prentice Hall; 2013.
25. Capon J. High-resolution frequency-wavenumber spectrum analysis. Proceedings of the IEEE. 1969; 57(8):1408–18.
26. Malaysian communications and multimedia commission. SKMM-MCMC Annual Report; 2011. Available from: http://www.skmm.gov.my/skmmgovmy/media/General/pdf/
27. Saxena P, Kothari A. Performance analysis of adaptive beamforming algorithms for smart antennas. IERI Procedia, Elsevier. 2014; 10:131–7.